Emulsion processing of polymer-derived porous Si/C/(O) ceramic bodies

Vadym Bakumov, Marcus Schwarz, Edwin Kroke *

Institute of Inorganic Chemistry, TU Bergakademie Freiberg, Leipziger Strasse 29, 09596 Freiberg, Germany

Abstract

A novel route of miniemulsion processing was applied to preceramic polymers in order to fabricate porous Si/C/(O) bodies. Commercially available polysiloxane and polycarbosilane precursors and water were emulsified via intensive stirring or ultrasonication in the presence of surfactants, and subsequently shaped and cured in an autoclave. The resulting green bodies were dried and pyrolytically converted at 700 and 1050 °C under nitrogen into ceramic counterparts retaining their shape. A fine interconnected pore network derived from the aqueous phase allows escape of gaseous decomposition products during pyrolysis and avoids cracking. In the presence of transition metals such as Fe, Co, Ni or Pd nanofibers consisting of β-SiC/a-SiO$_2$ are formed. Effects of polymer viscosity and processing parameters on the microstructures, porosities and pore sizes of the resulting products were investigated by means of DLS, mercury porosimetry, SEM, TEM, XRD and FTIR.
© 2009 Elsevier Ltd. All rights reserved.

Keywords: Shaping; Templating; Porosity; Carbides; Substrates

1. Introduction

Amphiphiles are routinely used for templating of inorganic materials, e.g. for the synthesis of mesoporous silica-based MCM-41, SBA-15 and other materials.[1] The approach offers control over porosity, size and morphology. Despite the tremendous interest for this topic, the majority of investigated materials are restricted to oxide systems based predominantly on silica- and transition metal oxides. Although bearing potential as adsorption, (photo-) catalytic and refractory materials, they have modest high temperature and chemical resistance, and current challenges for functional and high-performance structural materials for severe conditions are anticipated to be addressed by non-oxide ceramics.

Due to the versatility of shaping techniques available for polymers, the polymer-derived-ceramic route (PDC) is a powerful method leading to SiC,[2a] Si/(B)/(C)/N[2b] or Si/C/O[2c] amorphous and crystalline ceramics.[2] Powders, coatings, fibers, matrices of fiber-reinforced CMC and MEMS are considered as the most suitable area for PDC application. Although several polymeric precursors are already commercially available, the critical draw-backs of PDC processing for large bodies are cracks caused by degassing and shrinkage during pyrolysis. An approach to overcome this problem is the application of active and/or passive fillers that compensate shrinkage and relief stresses exerted during pyrolytic ceramisation.[3] The fabrication of ceramic foams via PDC routes does not encounter the problem of crack formation and is in focus of intensive and increasing research.[4,5] The reasons for successful crack-free pyrolysis are interconnected pores acting as channels for gaseous by-products. Potential applications of such foams include filters, membrane supports, refractory materials, etc. Another aspect of fine porosity is the large specific surface area being interesting for accommodating, e.g. catalytic or antibacterial nanoparticles or growth of nanotubes and nanofibers. The application of porous non-oxide ceramics in high temperature catalysis, e.g. fuel reforming, should benefit not only from the low self-diffusion coefficients precluding pore closure but also from high mass and heat flux transfer rates. This is especially the case for silicon carbide based PDC due to the high thermal conductivity of SiC.[2a] Porous Si/C/E membrane/catalyst supports withstand large pressure drops caused by gas flux because of the high strength of silicon carbide.[6] Examples for polymer-derived SiC catalytic supports[7] and polymer-derived SiC, Si/C/N, Si/B/C/N permselective membranes[8,9] have been reported recently.

Porous PDC ceramics are fabricated mostly via direct chemical foaming techniques, usually utilizing polyurethane

* Corresponding author. Tel.: +49 3731 39 3174; fax: +49 3731 39 4058.
E-mail addresses: kroke@chemie.tu-freiberg.de,
edwin.kroke@chemie.tu-freiberg.de (E. Kroke).

as blowing agent which decomposes under heat treatment.[10] The voids are created by the formation of volatile decomposition products prior or simultaneously with cross-linking of the precursor.[11] The cell size of the resulting foam varies usually in the range of 5 μm to 0.5 mm. Carbon dioxide as well as other gases can be applied for direct physical foaming.[12]

Replica techniques are based on the impregnation of porous templates with ceramic precursors or slurries followed by thermal treatment. The size, morphology and volume fraction of pores depend mainly on the used template, which can be synthetic, e.g. PU foam,[13] or natural, e.g. wood,[14] as well as on the precursor properties.

In the group of sacrificial template methods molding is accomplished using a mixture of a precursor and a sacrificial phase via pressing, slip-, tape- or direct casting, or impregnation. To obtain highly porous structures dense packed beads are used as templates. The latter method has the advantage of regularly oriented struts and highly homogeneous pore size distributions of the products. In Refs. [6,15] the porous ceramics are negative replica of polymer or silica microbeads used as sacrificial fillers. Expandable microspheres can be utilized for direct chemical foaming being a sacrificial template at the same time.[16] A comprehensive review on synthesis of macroporous ceramics is given in Ref. [17].

Mesoporous materials were also demonstrated to be effective sacrificial templates for nanostructuring of preceramic polymers. Mesoporous silica-based materials[18–20] and alumina[21] are traditionally used hosts, which however must be etched after ceramisation of the precursor. This etching step is costly in terms of time consumption and usually associated with dangerous chemicals (HF). First reports on direct PDC templating utilize self-assembling block-copolymers as structuring agents[22,23] and grafting non-miscible polymeric fragments (polyisoprene) to the polymeric precursor, which causes a spatial nanodomain separation resulting in porous Si/C/O.[24]

The stabilisation of oil/water interfaces with surfactants has also potential for structuring of polymer-derived ceramics. The emulsion droplets can be used as templates/microreactors for polymerisation reactions[25,26] and colloid synthesis,[27] which govern the final particle size. Depending on the particle size (crude) turbid unstable emulsions (few microns) and thermo-dynamically stable translucent microemulsions (10–40 nm) are discerned. The latter class suffers from high surfactant quantities and the necessity of dialysis. The third class – entropy-stabilized miniemulsions – can be produced by applying high shear rates and/or phase inversion.[28,29] Indeed, if emulsification does not occur spontaneously, miniemulsions can be obtained under the high shear of ultrasound,[30] which is increasingly used in material science.[31] Here we apply an earlier reported emulsion processing technique[32] to a polycarbosilane SiC precursor and extend the method to the fabrication of macroporous non-oxide ceramic bodies. The aim of the present study was the fabrication of intact polymer-derived ceramic bodies with submicron-scaled transient porosity. This is attained by processing more concentrated (30–70 wt.%) precursor-water-surractant mixtures as compared to the previous work[32] mixtures with water and surfactant. Cross-linking above 100 °C in an autoclave transforms the mixture to the rigid form. The percolation of precursor droplets ensures integrity of the resulting body, whereas continuous water phase acts as a sacrificial template for transient porosity. The advantage of this new method is the fine macro-porosity which can be controlled by precursor and processing parameters (composition, viscosity, shear rate, temperature, the sequence of processing steps).

2. Experimental

2.1. Synthetic technique

In a typical synthesis "oil" and "water" phases were mixed in definite volume proportions (Table 1, "oil content"). First phase (either "oil" or "water") was added dropwise to the second one, which was exposed to continuous sonication with ultrasound applying a power of 120 W (Sonopuls HD 2200 ultrasound generator, BANDELIN Electronic GmbH & Co. KG, Berlin, Germany). The temperature between 60 and 80 °C was kept during sonication. Alternatively, a high-performance stator-rotor homogenizer "Silent crusher M" (Heidolph Instruments GmbH & Co. KG, Schwabach, Germany) at stir rates up to 20,000 rpm was used. After addition of the second phase sonication was continued for another 3 min. Centrifugation was applied to eliminate bubbles of entrapped air. The emulsion was poured into a Teflon-

Table 1
Sample designation, emulsion compositions, processing parameters and porosities of MK- and SMP-derived Si/C/(O)-specimens.

Sample designation	"Oil" content	Surfactant	Processing technique/remarks	Porosity of ceramic	Porosity of green body
MK60P1	60%	3 wt.% PEO–PPO–PEO	Water added to oil, MK:toluene = 1:1 vol.	–	
MK60P2	60%	3 wt.% PEO–PPO–PEO	Water added to oil MK:toluene = 5:1 vol. 30 min of sonication	40%	~40%
MK66P	66%	3 wt.% PEO–PPO–PEO	Oil added to water MK:toluene = 5:1 vol.	15%	
SMP64S	64%	3 wt.% SDS	Oil added to water	30%	25%
SMP46P	46%	2 wt.% PEO–PPO–PEO	Water added to oil	52%	46%
SMP50S	50%	2 wt.% SDS	Oil added to water	21%	12%
SMP50P1	50%	3 wt.% PEO–PPO–PEO	Cross-linking at 153 °C	–	
SMP50P2	50%	3 wt.% PEO–PPO–PEO	Cross-linking at 163 °C	–	
SMP50P3	50%	2 wt.% PEO–PPO–PEO	Silent crusher M	52%	47%

lined autoclave, sealed, heated and kept overnight at a determined temperature for cross-linking. If not specified otherwise, the cross-linking temperature was 150 °C. The "oil" phase consists of polyallylhydridocarbosilane (PCS) STARFIRE® SMP-10 (Starfire® Systems, Malta, NY, USA) for SiC-based ceramics. For products in the Si/C/O system 8 g of WACKER-BELSIL® poly(methylsilsesquioxane) PMS MK (Wacker Chemie AG, Munich, Germany) and 80 mg of the cross-linking agent zirconium (IV) acetylacetonate were dissolved in 2 g of toluene. Alternatively, if formation of nanofibers is desired (next section), iron (III) or cobalt (III) acetylacetonate can be used. The "water" phase is an aqueous solution of surfactant (2–5 wt.%). Anionic (sodium dodecylsulfate, SDS), cationic (dodecyl trimethylammoniumbromide, DTAB) or non-ionic (poly(ethylene-glycol)–*block*–poly(propylene-glycol)–*block*–poly(ethylene-glycol) PEO–PPO–PEO with $M_n = 14,600$ g/mol from Sigma–Aldrich) surfactants were used. The examined compositions and obtained porosity data are summarized in Table 1.

After cooling down to room temperature water-containing green bodies were released and immersed in deionized water for 2 h, and air-dried for 24 h. In order to catalyze more extensive formation of nanofibers, small amount (ca. 1 mg/ml) of $NiCl_2$ was added to water. Dry bodies were finally pyrolyzed in quartz Schlenk-tubes with a tube furnace Heraeus Ro 4/50 (Heraeus Instruments GmbH, Hanau, Germany) under flowing nitrogen by heating to 700 and 1050 °C, respectively, applying a heating rate of 40 °C/h and a holding time of 1 h in all cases.

2.2. Characterisation

X-ray diffraction (XRD) data were collected on a Guiner-type diffractometer Huber G670 (HUBER Diffraktionstechnik GmbH & Co. KG, Rimsting, Germany) with an image plate, using Cu Kα1 radiation (0.154056 nm). Scanning electron microscopy (SEM) was performed on a LEO1530 FEG (Karl Zeiss NTS GmbH, Oberkochen, Germany) with accelerating voltage of 12–20 kV. A Zeiss Libra 120 EFTEM (Carl Zeiss NTS GmbH) transmission electron microscope (TEM) was used for the TEM investigation. Fourier transform infrared spectroscopy (FTIR) was performed with a Perkin Elmer System 2000 spectrometer (PerkinElmer Life and Analytical Sciences, Inc., Wellesley, USA) using the standard KBr pellet technique. Nitrogen adsorption data were obtained with a Micromeritics ASAP 2000 system (Micromeritics Instrument Corp., Norcross, USA) and evaluated using the ASAP 2010 software package. The dynamic light scattering (DLS) measurements were conducted on emulsions diluted with deionized water (1:20) using a Zetasizer Nano ZS (Malvern Instruments Ltd., Worcestershire, United Kingdom). ^{29}Si solid state nuclear magnetic resonance (NMR) spectra acquisition was performed on BRUKER Avance™ 400 MHz WB (Bruker BioSpin GmbH, Rheinstetten, Germany) with a resonance frequency of 79.51 MHz using magic-angle spinning (MAS) at 5 kHz without cross-polarization (CP). The chemical shift values are referenced to tetramethylsilane (TMS). Mercury pressure porosimetry was performed on a Thermo Scientific Pascal (Thermo Fisher Scientific Inc., MA, USA).

3. Results and discussion

Within the present work two largely moisture-insensitive commercially available precursor polymers were examined with respect to their suitability for emulsion templating. The first one, the polysilsesquioxane "MK", cross-links via polycondensation reactions, whereas the second one, the polycarbosilane "SMP" contains allyl groups which cross-link via slow hydrosilation. Being confined within the "oil" phase of ultrasonically assisted emulsification and thermally cured, the polymer body inherits porosity from the "water" phase and the shape from the autoclave Teflon liner.

To be suitable for emulsion processing the preceramic polymer, surfactant and processing steps should meet some requirements. The polymer should be liquid or at least highly soluble in non-polar solvents. It should be water insensitive and contain functional groups responsible for cross-linking. The hydrophilic–lypophilic balance (HLB) of the surfactant should be high enough to determine high cloud temperatures (>100 °C) and withstand autoclave curing. An aim of the present work was to produce intact PDC bodies with significant porosity (>30%). In the following the influence of the composition, processing conditions and cross-linking temperature on the fabrication of porous PDC bodies are discussed.

3.1. Polysilsesquioxane-derived porous Si/C/O bulk bodies

To be processable via emulsion routes the solid polysilsesquioxane "MK" has to be dissolved in a solvent which is immiscible with water. The amount of solvent should be minimized, since during its evaporation after cross-linking, the lost volume (shrinkage) causes tensile stresses within the matrix and cracks (Fig. 1). However, excellent miscibility of MK with toluene allows dissolving four weight parts of polymer in one weight part of toluene at room temperature and more than six parts above 60 °C, which reduces the shrinkage during drying and leads to crack-free specimens.

The optimal microstructure consists of two continuous interpenetrating phases. The "oil" phase contains the polymer, which is the building material of the porous body. The aqueous phase determines the transient porosity needed to expel gaseous by-products during pyrolysis. The transition to the bi-continuous phase (Fig. 2, left) from w/o is characterized by increase in viscosity and electrical conductivity. However the high viscosity limits the efficiency of shear forces (e.g. sonication), which results in non-homogeneity of specimens as well as in large struts and pores.

The amount of homogeneously distributed water and hence the porosity of the resulting ceramics is limited by phase inversion. By slow addition of water to the "oil" phase under sonication, a porosity above 40% can be obtained. However, further addition of water to the viscous phase causes phase inversion and o/w formation. In this case, and if the stabilisation forces are short-reaching (sterical stabilisation by PEO–PPO–PEO), the crude droplets coagulate quickly at ambient temperature and precipitate due to the relatively high density of the MK polymer (1.2 g/cm^3). In the case of charge stabilisation, water separation

Fig. 1. Green bodies with toluene content within the "oil" phase of 50% – MK60P1 (left) and 17% – MK60P2 (right). Scale bar is 1 cm.
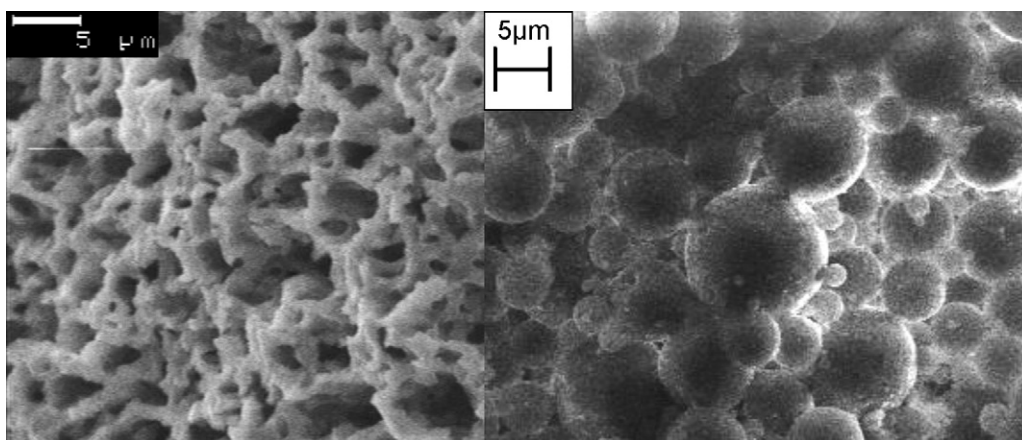

Fig. 2. SEM micrographs of emulsion-processed polysilsesquioxane-derived Si/C/O ceramics: bi-continuous phase of sample MK60P2 (left) and spherical o/w morphology of sample MK66P (right).

does not occur immediately, but the green body shrinks during drying. For both types of surfactants, dense packed beads form the resulting body (Fig. 2, right) with porosity around 10–15%. Details of the polymer-to-ceramic transformation of emulsion-processed polysilsesquioxane, elemental composition and chemical–structural characterisation of the ceramic products can be found elsewhere.[32]

3.2. Polycarbosilane-derived porous SiC bulk bodies

The as-received polymer "SMP" was characterized by NMR and FTIR spectroscopy (not shown here). The spectral features of this polycarbosilane (PCS) correspond well with the literature.[33]

High shear and phase inversion are the two general approaches to create miniemulsions.[29,34] The choice of the processing method becomes especially important, since high viscosity of precursors limits the efficiency of high shear. The size of the obtained droplets is in the range of 200–1000 nm (Fig. 3). This is much larger than that of low viscous systems described in Ref. [32].

Here we compare two ultrasonic-assisted methods: direct sonication of o/w emulsion and dropwise addition of water under ultrasonic treatment until phase inversion occurs (detected by a strong drop of electrical resistivity). It turned out that the former approach is preferable, since it led to finer droplets and finer porosity (Figs. 4 and 5). It can be concluded from this result that the viscosity of the continuous phase has much higher impact on the damping of shear than that of the dispersed phase.

Attempts to obtain bi-continuous PCS/water phases either via direct sonication or via phase inversion (concentration or temperature induced) led to networks of partially fused particles (Fig. 4). This fusion likely proceeds already in liquid state during cross-linking, since pyrolysis causes increase of porosity (Table 1). Normally, the particles and the necks connecting
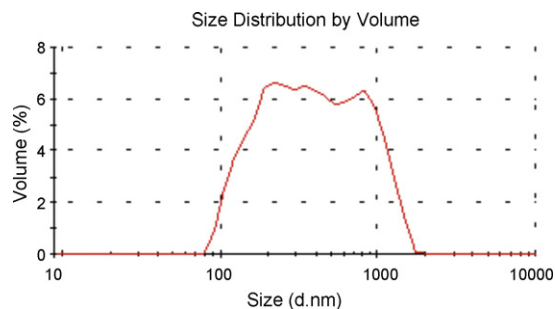

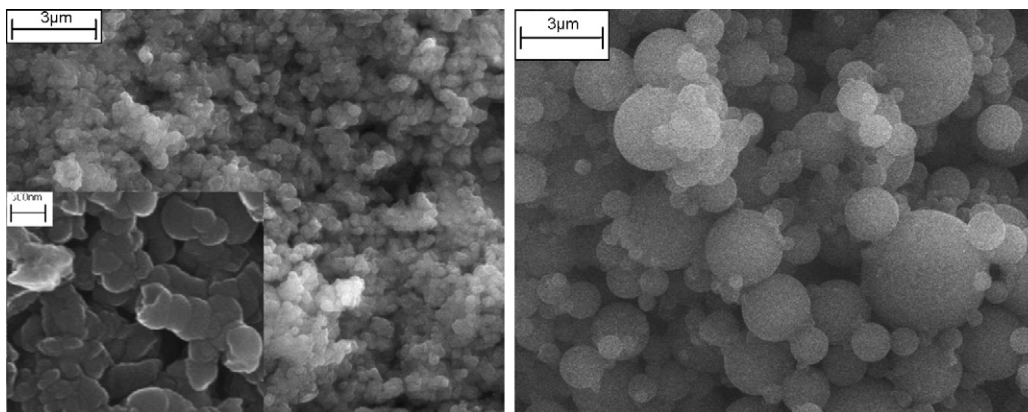Fig. 3. Droplet size distribution by volume of PCS emulsion measured by means of DLS.

Fig. 4. SEM micrographs of emulsion processed PCS-derived porous ceramics; left: SMP64S, PCS content 64%, o/w, continuous sonication, bar scale of the inset 300 nm; right: SMP46P, water content was increased dropwise under sonication until phase inversion occurred at 46% of PCS.
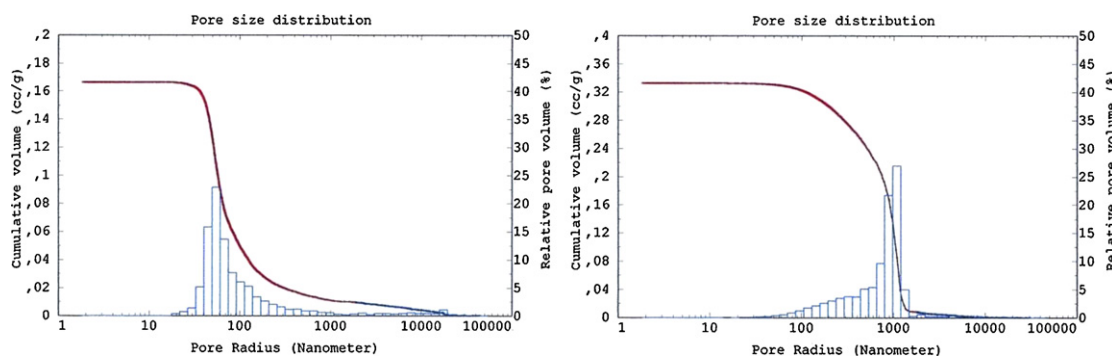

Fig. 5. Pore size distribution of emulsion processed PCS-derived porous ceramics measured by mercury pressure porosimetry; left: SMP64S, PCS content 64%, resulting open porosity 30%, o/w, continuous sonication; right: SMP46P, PCS content was decreased dropwise under sonication until phase inversion occurred at 46%, resulting open porosity 52%.

them can be discerned, the latter, being cross-linked withstand pyrolytic transformation, retaining their shape (Fig. 4, inset). One of the possible reasons for the difference between both polymers (compare Figs. 4 and 2) is the higher viscosity of the concentrated MK solution compared to the PCS precursor. It is known, that for nano-droplet formation applied shear stresses must exceed the Laplace pressure and elongate large droplets.[34] The shear of sonication is obviously insufficient to produce significant elongation and initiation of capillary instability. This may be attributed to a high damping of the ultrasound by the viscous starting continuous phase.

Since miniemulsions are kinetically stabilized, sequences and parameters of processing steps are essential. In particular, we observed that surfactants with high HLB values (>25) can stabilize o/w miniemulsion with "oil" contents as high as 67%, if "oil" is continuously added to "water" under shear force. In contrary, for the same components, the catastrophic phase inversion from w/o to o/w occurs at an "oil" content below 47% if "water" is slowly added to "oil" under sonication (see below). Such retention is well expressed in the case of polymeric surfactants, which adsorb irreversibly on the water/oil interface causing a high energy barrier for phase inversion. The irreversibility can be demonstrated for the example of electrophoretic mobility of polysilsesquioxane miniemulsions (Fig. 6). PEO–PPO–PEO adsorbs preferably on the "water/oil" interface of the charge-

stabilized emulsion droplets, substituting the cationic surfactant, which results in a zeta-potential of nearly zero.

The effect of cross-linking temperatures is strongly related to the cloud point of the applied surfactant. A small increase of temperature (10 °C) leads to the inverse emulsion formation and to pore closure (Fig. 7). This observation can be explained in terms of coagulation and dehydration of PEO chains above the cloud point. As a result, the surfactant loses its amphiphilic properties. The as-cured bodies with closed porosity retained their shape, but contained numerous cracks.

The surfactant SDS does not reveal a cloud point in the tested temperature range (RT–170 °C), therefore the spherical morphology of the polymer droplets is retained, and the result-
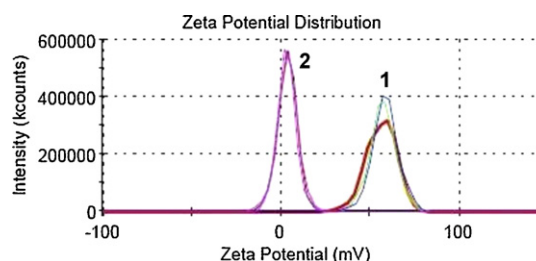

Fig. 6. Zeta-potential distribution of emulsions stabilized by DTAB before (1) and after addition of PEO–PPO–PEO (2).
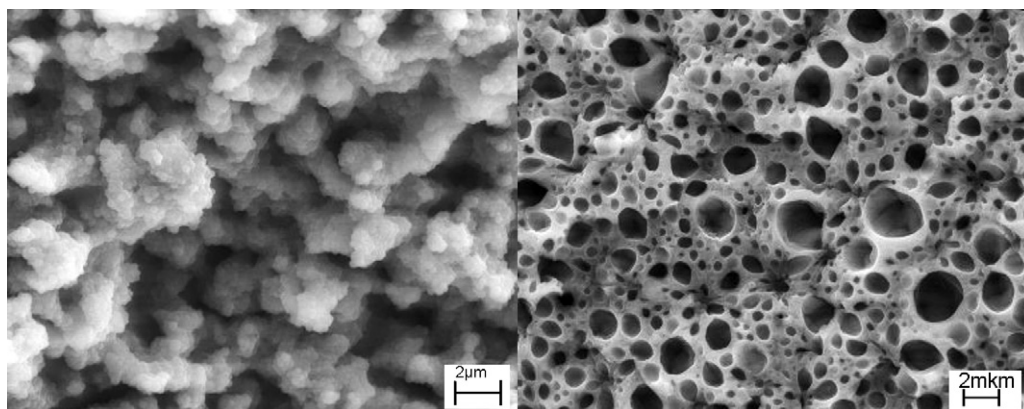
Fig. 7. SEM micrographs of emulsion-processed (water content 50%) PCS-derived Si/C/(O) samples using PEO–PPO–PEO (3 wt.%) as surfactant: cross-linking temperature SMP50P1: 153 °C (left) and SMP50P2: 163 °C (right).

ing ceramic porous bodies resemble in their microstructure the packed beads (Fig. 4). At "oil" fractions above 50% deformation of particles was observed (Fig. 4, left). Remarkable is the fact that the emulsions with oil contents below 50% resulted in porosities as low as 10% after shrinkage during drying, whereas more concentrated emulsions (62–66%) did not reveal significant shrinkage and preserved high porosities (30–35%). This can be caused by the rigid structure of the viscous concentrated o/w starting solution and absence of free volume needed for particles to rearrange to build a densely packed framework. These suggestions coincide with structural transitions of emulsions upon concentrating,[34] but need further systematic investigation. As the most probable driving force for shrinkage upon drying we consider the Laplace pressure directed toward the "water", which possesses negative curvature. Small droplet size and hence (by homogeneous distribution) small pore size of the sample SMP50S as compared to SMP46P and SMP50P3 results in sufficient capillary force within the interparticle voids and pushes them together, when water evaporates (Table 1).

The shear forces of the stator-rotor system (300 s^{-1}) result in larger particles and pores (Fig. 8). The specimens do not shrink retaining the predetermined porosity. The presence of
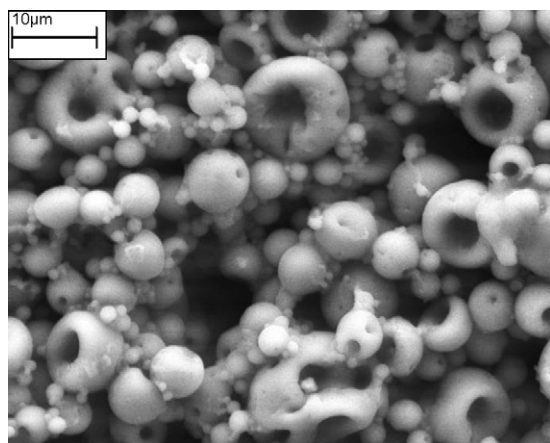
bowl-like structures in PCS-derived SiC, which were observed earlier for Si/C/O-materials,[32] implies the irrelevance of the solvent to their formation and is most likely attributed to the nature of shear forces exerted by the stator-rotor. Dried green bodies were pyrolytically converted to ceramic specimens with yields of 73%, preserving their shape (Fig. 9).

Investigation of the chemistry of polymer-to-ceramic transition of the commercial carbosilane SMP used in this study can be found elsewhere.[6,35] Here we touch only a few aspects of purity and microstructure. In FTIR as well as in ^{29}Si NMR spectra (Figs. 10 and 11) the typical features of polymer-derived SiC ceramics are detected. The broad absorption band as well as broad reflexes in the XRD patterns (Fig. 12) are a result of a low degree of ordering indicating that the products are largely amorphous. XRD patterns obtained after pyrolysis at 700 °C show a peak at 6.8° 2θ. The corresponding lattice distance of 1.2–1.3 nm can be attributed to a small amount of micropores left behind after evaporation of volatile species. However, microporosity was not detected by means of nitrogen physisorption, which may be explained by the closed character of the micropores. In the final ceramics formed at 1050 °C the pores disappeared due to sintering and diffusion processes as indicated by the absence of XRD peaks at low 2θ values for the corresponding samples

Fig. 8. SEM micrograph of PCS-derived porous ceramics processed under shear of a stator-rotor system (sample SMP50P3).

Fig. 9. Emulsion-processed polymer-derived SiC bodies with porosities of 10–35%.
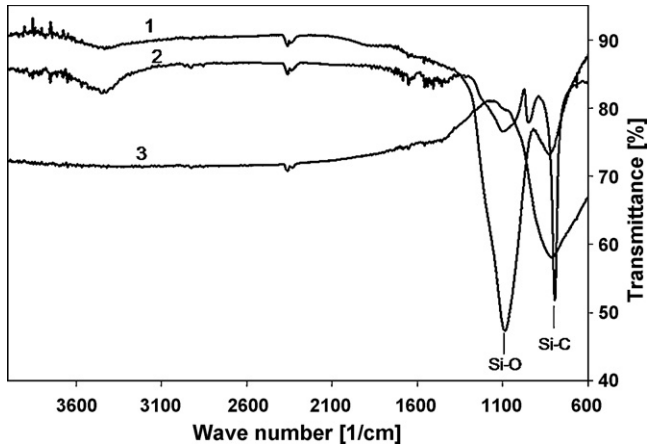
Fig. 10. FTIR spectra of MK-derived ceramics (1), Si/C/(O) nanofibers (2) and PCS-derived ceramics (3).
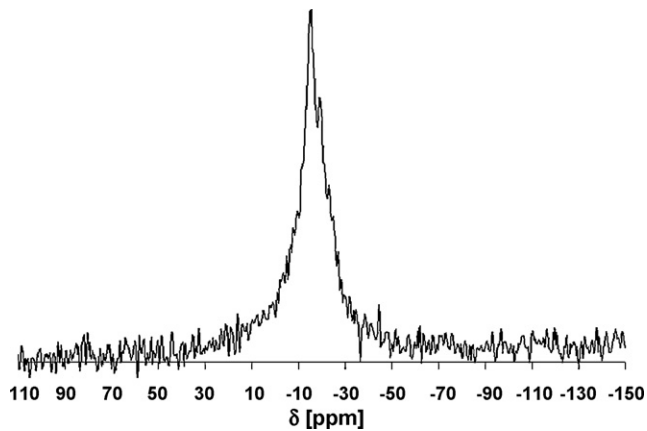

Fig. 11. ^{29}Si NMR spectrum of emulsion-processed PCS-derived SiC.

(Fig. 12). Besides, at 1050 °C crystallization of nanocrystalline β-SiC begins. Similar results have been reported recently on crystallization of polycarbosilane-derived SiC.[35]

3.3. Formation of Si/C/(O) nanofibers

Another aspect of porosity is free evolution of silicon-containing gaseous species inside the pores. This can lead to
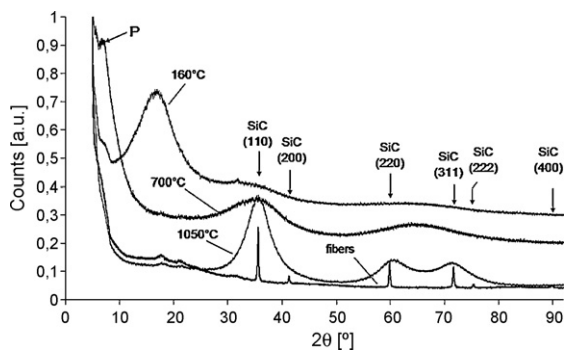

Fig. 12. X-ray diffractogramms of Si/C/(O) nanofibers, and emulsion-processed polycarbosilane treated at various temperatures: as cured at 160 °C, transformed to hybride material at 700 °C and ceramised via annealing at 1050 °C for 1 h.
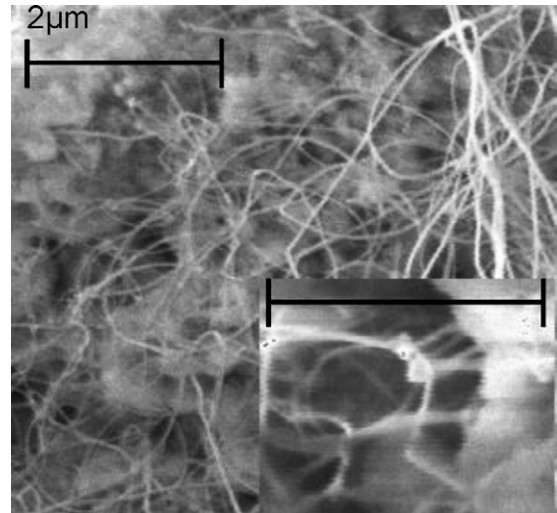

Fig. 13. SEM micrographs of Si/C/(O) fibers formed within a porous PDC bulk body at 1050 °C. Scale bar of inset is 1 μm.

the formation of nanofibers on the surface as well as within the voids of porous PDC bodies (Fig. 13). Factors that promote fiber formation are the presence of traces of transition metals (Fe, Co, Ni, Pd), slow flow rates of nitrogen during pyrolysis and residual surfactants bound to the surface. The catalytic effect of the metal is more pronounced if it is introduced via the "water" phase (addition of <0.1% of NiCl$_2$ to the aqueous phase, contact with steel), than if it was present in the "oil" phase (e.g. as iron (III) or cobalt (III) acetylacetonates). The surfactants increase the amounts of carbon in the C-poor polysilsesquioxane precursor.

The FTIR spectrum of the nanofibers (Fig. 10) reveals a strong absorption band at 794 cm^{-1} which is assigned to Si–C valence vibrations and a smaller band associated with Si–O bonds (1080 cm^{-1}). The sharpness of the Si–C band (compare with that of PCS-derived SiC bulk in Fig. 10) can be attributed to a high degree of crystallinity, which is confirmed by XRD (Fig. 12). TEM also reveals crystalline regions with ordered faces within the fiber (Fig. 14). The nanofibers are also formed on
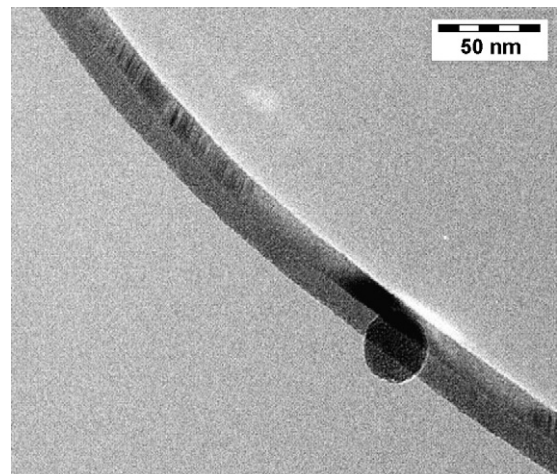

Fig. 14. TEM micrograph of a Si/C/(O) nanofiber formed within the pores of a PDC body.

a quartz substrate if it is put in close proximity to the porous body during pyrolysis. The latter observation indicates that vapour phase transport processes are responsible for the Si/C/(O) or β-SiC/SiO$_2$ nanofiber formation. The fact that the FTIR spectra of the nanofibers do not depend on the starting polymer (MK or PCS) and show the presence of Si–O bonds, indicates that oxygen is playing a crucial role for nanofiber formation. EELS measurements of the fiber (not shown here) proved the presence of silicon, carbon and oxygen. Therefore, silicon monoxide may be the responsible volatile silicon compound which reacts with carbon species to form Si/C/(O). These observations agree with a vapour–liquid–solid (VLS) mechanism proposed for the formation of nanofibers, additional information is provided in Ref. [36].

4. Conclusions

The polymer-to-ceramic approach was extended to the fabrication of bulk bodies with pore sizes in the range of 50 nm to 5 μm using emulsion processing. The presented method is based on templating of liquid, water-insensitive precursors in miniemulsions with subsequent cross-linking, drying and pyrolysis. Viscosity of the precursor, temperature and processing conditions are the critical parameters determining the resulting structure: porosity, pore size and morphology. High shear turns out to be more effective, when highly viscous precursors are dispersed in low viscous aqueous phases. The fine (interconnected) pores build tunnels for gaseous by-products avoiding crack formation during pyrolysis. Systematic optimization is needed to meet specific requirements for possible application such as filters, catalyst carriers or structural ceramic components. One of the advantages of the presented approach is the possibility to fabricate composites reinforced with metal wires or grids by introducing the latter into the green body, preferably before cross-linking. The observed formation of β-SiC/a-SiO$_2$ nanofibers in the pores bears potential in strengthening and toughening of bulk bodies as well as in affecting the pores size and surface area.

Acknowledgements

References

1. Hoffmann, F., Cornelius, M., Morell, J. and Froba, M., Silica-based mesoporous organic–inorganic hybrid materials. *Angew. Chem. Int. Ed.*, 2006, **45**, 3216–3251.

2. (a) Roewer, G., Herzog, U., Trommer, K., Mueller, E. and Fruehauf, S., Silicon carbide—a survey of synthetic approaches, properties and applications. *Struct. Bond.*, 2002, **101**, 59–135;
(b) Kroke, E., Li, Y.-L., Konetschny, C., Lecomte, E., Fasel, C. and Riedel, R., Silazane-derived ceramics and related materials. *Mater. Sci. Eng. R*, 2000, **26**, 97–199;
(c) Zank, G. A., Preceramic polymer—derived silicon oxycarbides. *Silicon-Contain. Polym.*, 2000, 697–726;
(d) Riedel, R., Mera, G., Hauser, R. and Klonczynski, A., Silicon-based polymer-derived ceramics: synthesis properties and applications—a review. *J. Ceram. Soc. Jpn.*, 2006, **114**, 425–444.

3. Greil, P., Near net shape manufacturing of polymer derived ceramics. *J. Eur. Ceram. Soc.*, 1998, **18**, 1905–1914.

4. (a) Colombo, P. and Hellmann, J. R., Ceramic foams from preceramic polymers. *Mater. Res. Innovat.*, 2002, **6**, 260–272;
(b) Scheffler, M. and Colombo, P., ed., *Cellular Ceramics: Structure, Manufacturing, Properties and Applications*. Wiley-VCH, Weinheim, Germany, 2005, 670 p.

5. Schmidt, H., Koch, D., Grathwohl, G. and Colombo, P., Micro-/macroporous ceramics from preceramic precursors. *J. Am. Ceram. Soc.*, 2001, **84**, 2252–2255.

6. Sung, I.-K., Mitchell, C. M., Kim, D.-P. and Kenis, P. J. A., Tailored macroporous SiCN and SiC structures for high-temperature fuel reforming. *Adv. Funct. Mater.*, 2005, **15**, 1336–1342.

7. Kockrick, E., Krawiec, P., Petasch, U., Martin, H.-P., Herrmann, M. and Kaskel, S., Porous CeOX/SiC nanocomposites prepared from reverse polycarbosilane-based microemulsions. *Chem. Mater.*, 2008, **20**, 77–83.

8. Nagano, T., Sato, K., Saitoh, T. and Iwamoto, Y., Gas permeation properties of amorphous SiC membranes synthesized from polycarbosilane without oxygen-curing process. *J. Ceram. Soc. Jpn.*, 2006, **114**, 533–538.

9. Völger, K. W., Hauser, R., Kroke, E., Riedel, R., Ikuhara, Y. H. and Iwamoto, Y., Synthesis and characterization of novel non-oxide sol–gel derived mesoporous amorphous Si–C–N membranes. *J. Ceram. Soc. Jpn.*, 2006, **114**, 567–570.

10. Fukushima, M., Zhou, Y., Miyazaki, H., Yoshizawa, Y., Hirao, K., Iwamoto, Y. *et al.*, Microstructural characterization of porous silicon carbide membrane support with and without alumina additive. *J. Am. Ceram. Soc.*, 2006, **89**, 1523–1529.

11. Colombo, P., Gambaryan-Roisman, T., Scheffler, M., Buhler, P. and Greil, P., Conductive ceramic foams from preceramic polymers. *J. Am. Ceram. Soc.*, 2001, **84**, 2265–2268.

12. Kim, Y.-W., Kim, S.-H., Xu, X., Choi, C.-H., Park, C. B. and Kim, H.-D., Fabrication of porous preceramic polymers using carbon dioxide. *J. Mater. Sci. Lett.*, 2002, **21**, 1667–1669.

13. Nangrejo, M. R., Bao, X. and Edirisinghe, M. J., Preparation of silicon carbide-silicon nitride composite foams from pre-ceramic polymers. *J. Eur. Ceram. Soc.*, 2000, **20**, 1777–1785.

14. Zollfrank, C., Kladny, R., Sieber, H. and Greil, P., Biomorphous SiOC/C-ceramic composites from chemically modified wood templates. *J. Eur. Ceram. Soc.*, 2004, **24**, 479–487.

15. Lee, S.-H. and Kim, Y.-W., Processing of cellular SiC ceramics using polymer microbeads. *J. Korean Ceram. Soc.*, 2006, **43**, 458–462.

16. Jang, D.-H., Kim, Y.-W., Song, I.-H., Kim, H.-D. and Park, C. B., Processing of highly porous, open-cell, microcellular silicon carbide ceramics by expansion method using expandable microspheres. *J. Ceram. Soc. Jpn.*, 2006, **114**, 549–553.

17. Studart, A. R., Gonzenbach, U. T., Tervoort, E. and Gauckler, L. J., Processing routes to macroporous ceramics: a review. *J. Am. Ceram. Soc.*, 2006, **89**, 1771–2178.

18. Krawiec, P., Geiger, D. and Kaskel, S., Ordered mesoporous silicon carbide (OM–SiC) via polymer precursor nanocasting. *Chem. Commun.*, 2006, 2469–2470.

19. Yoon, T.-H., Lee, H.-J., Yan, J. and Kim, D.-P., Fabrication of SiC-based ceramic microstructures from preceramic polymers with sacrificial templates and lithographic techniques—a review. *J. Ceram. Soc. Jpn.*, 2006, **114**, 473–479.

20. Park, K.-H., Sung, I.-K. and Kim, D.-P., A facile route to prepare high surface area mesoporous SiC from SiO$_2$ sphere templates. *J. Mater. Chem.*, 2004, **14**, 3436–3439.

21. Ginzburg-Margau, M., Fournier-Bidoz, S., Coombs, N., Ozin, G. A. and Manners, I., Formation of organometallic polymer nanorods using a nanoporous alumina template and the conversion to magnetic ceramic nanorods. *Chem. Commun.*, 2002, 3022–3023.

22. Kamperman, M., Garcia, C. B. W., Du, P., Ow, H. and Wiesner, U., Ordered mesoporous ceramics stable up to 1500 °C from diblock copolymer. *J. Am. Chem. Soc.*, 2004, **126**, 14708–14709.

23. Wan, J., Alizadeh, A., Taylor, S. T., Malenfant, P. R. L., Manoharan, M. and Loureiro, S. M., Nanostructured non-oxide ceramics templated via block copolymer self-assembly. *Chem. Mater.*, 2005, **17**, 5613–5617.

24. Chan, V. Z.-H., Hoffman, J., Lee, V. Y., Iatrou, H., Avgeropoulos, A., Hadjichristidis, N. *et al.*, Ordered bicontinuous nanoporous and nanorelief ceramic films from self assembling polymer precursors. *Science*, 1999, **286**, 1716–1719.

25. Van, H. A., *Chemistry and Technology of Emulsion Polymerisation*. Blackwell Publishing Ltd., 2005.

26. Mecking, S., Monteil, V., Huber, J., Kolb, L. and Wehrmann, P., Synthesis of very small polymer particles by catalytic polymerization in aqueous systems. *Macromol. Symp.*, 2006, **236**, 117–123.

27. Lopez-Quintela, M. A., Rivas, J., Blanco, M. C., Tojo, C., Liz-Marzan, L. M. and Kamat, P. V., ed., *Nanoscale Materials: Synthesis of Nanoparticles in Microemulsions*. Springer, US, 2003, pp. 135–155.

28. Tadros, T. F., *Applied Surfactants: Principles and Applications*. Wiley-VCH, Weinheim, Germany, 2005, 634 p.

29. Sajjadi, S., Nanoemulsion formation by phase inversion emulsification: on the nature of inversion. *Langmuir*, 2006, **22**, 5597–5603.

30. Mecking, S., Polymer dispersions from catalytic polymerization in aqueous systems. *Colloids Polym. Sci.*, 2007, 605–619.

31. Suslick, G. J., Applications of ultrasound to materials chemistry. *Ann. Rev. Mater. Sci.*, 1999, **29**, 295–326.

32. Bakumov, V., Schwarz, M. and Kroke, E., Emulsion processing and size control of polymer-derived spherical Si/C/O ceramic particles. *Soft Mater.*, 2007, **4**, 287–299.

33. Puerta, A. R., Remsen, E. E., Bradley, M. G., Sherwood, W. and Sneddon, L. G., Synthesis and ceramic conversion reactions of 9-BBN-modified allyl-hydridopolycarbosilane: a new single-source precursor to boron-modified silicon carbide. *Chem. Mater.*, 2003, **15**, 478–485.

34. Mason, T. G., Wilking, J. N., Meleson, K., Chang, C. B. and Graves, S. M., Nanoemulsions: formation, structure, and physical properties. *J. Phys.: Condens. Matter*, 2006, **18**, 635–666.

35. Li, H., Zhang, L., Cheng, L., Wang, Y., Yu, Z., Huang, M. *et al.*, Polymer–ceramic conversion of a highly branched liquid polycarbosilane for SiC-based ceramics. *J. Mater. Sci.*, 2008, **43**, 2806–2811.

36. Berger, A., Pippel, E., Woltersdorf, J., Scheffler, M., Cromme, P. and Greil, P., Nanoprocesses in polymer-derived Si–O–C ceramics: electronmicroscopic observations and reaction kinetics. *Phys. Status Solidi A*, 2005, **202**, 2277–2286.